Order online now!

www.rockland.com
tech@rockland.com
+1 484.791.3823

Datasheet for RT-T297

Rat Tail

Overview

Description:	Rat Tail - RT-T297
Item No.:	RT-T297
Size:	50 Pack
Applications:	Cellular Assay
Origin:	Rat

Product Details

Synonyms:	Rat tissue, Rat Collagen, Rat Type I Collagen
Species of Origin:	Rat

Application Details

Suggested Applications:	Cellular Assay (Based on references)

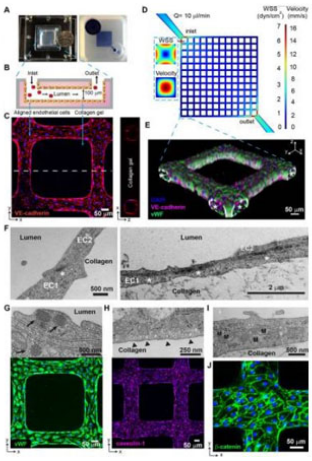
Formulation

Physical State:	Tissue

Shipping & Handling

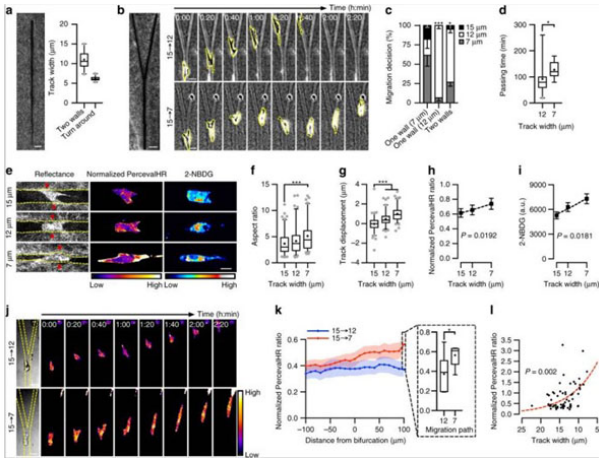
Shipping Condition:	Dry Ice
Storage Condition:	Store tissue at -20° C or colder prior to use.
Expiration:	No expiration date is given for this product if properly stored.

Images



Figure

Characterization of 3D brain microvessels. (A) (Left) Photo of an assembled 3D microvessel device with a dime (diameter, 17.9 mm). (Right) 3D microvessels perfused with food dye. (B) Schematic cross-sectional view of the 3D microvessels. (C) Immunofluorescence assay (IFA) z-projection of confocal sections of a 3D brain microvessel (left) and cross-sectional view (right) labeled with anti-VE-cadherin (red) and DAPI (blue). (D) Mid-plane flow velocity (z = 50 µm) and estimated WSS (z = 0 µm) distributions in the grid geometry, simulated with COMSOL prior to collagen remodeling by HBMEC (see Materials and Methods). Inlaid cross-sectional views represent the lumen at the first branch after the inlet. (E) 3D reconstruction of a grid portion. Colors indicate anti-VE-cadherin antibody (red), anti-VWF antibody (green), and DAPI (blue). Asterisk, lumen. (F) Transmission electron microscopy (TEM) showing endothelial junctions and focal contacts. EC1 and EC2, endothelial cells 1 and 2; asterisk, electron-dense contacts. (G) TEM showing Weibel-Palade bodies (arrows, top) and IFA z-projection of VWF (green, bottom). (H) TEM image of polarized caveolae (arrowheads, top) and IFA z-projection of caveolin-1 (magenta, bottom). (I) TEM image reveals high mitochondrial (M) content of HBMEC. (J) IFA z-projection of adherens junctions stained with anti-β-catenin antibody (green). Nuclei in panels G, H, and J were stained with DAPI (blue). Rat tail (p/n RT-T297). Fig 1. PMID: 31138740.



Figure

Spatial confinement influences migration decision-making, cellular ATP:ADP ratio, and glucose uptake. a Confocal reflectance image of a tapered collagen microtrack, and track width when cells contact two side walls of the microtrack or turn around and reverse migration direction (n = 20 cells). b Confocal reflectance image of a Y-shaped collagen microtrack and time-series images of decision-making during migration in Y-shaped microtracks (cell body outlined in yellow). c Final migration choice of cells based on cell-matrix contact before reaching the bifurcation (n = 34, 29, 41 cells for one wall (7 µm), one wall (12 µm), or two walls). d Time taken for cells touching two walls to pass through the bifurcation and enter a branch (n = 29 cells). e Confocal reflectance images of microtrack structure, and normalized PercevalHR ratio and 2-NBDG heatmaps of cells in each microtrack (yellow lines show microtrack walls; red arrowheads show areas of matrix displacement around the cell body). f, g Quantification of cell body aspect ratio (f) and track displacement (g) for cells in 15, 12, and 7 µm microtracks (n = 95, 96, and 91 cells, respectively). h, i Normalized PercevalHR ratio (n = 95, 96, and 91 cells, respectively) (h) and 2-NBDG uptake (n = 54, 40, and 56 cells, respectively) (i) for cells in 15, 12, and 7 µm microtracks. j Intracellular ATP:ADP ratio (normalized PercevalHR ratio) during decision-making in Y-shaped microtracks (yellow lines show microtrack walls). k Quantification of normalized PercevalHR ratio as a function of distance from the bifurcation and after final migration choice (n = 10 cells for 12 µm path, 5 cells for 7 µm path). l Normalized PercevalHR ratio in tapered collagen microtracks (n = 62 cells). Data shown as median ± interquartile range (box), 5th–95th percentiles (whiskers), and mean (+) (a, d, f, g, k), or mean ± s.e.m. (c, h, i); dashed lines show exponential growth; Clopper–Pearson confidence interval for observed proportion (c), two-tailed Mann–Whitney test (d, f, g, k), or extra sum-of-squares F-test (h, i, l); *P < 0.05, **P < 0.01, ***P < 0.001. Scale bar, 50 µm (a, b), 25 µm (b, j), and 15 µm (e). Rat tail (p/n RT-T297). Fig 1. PMID: 31519914.

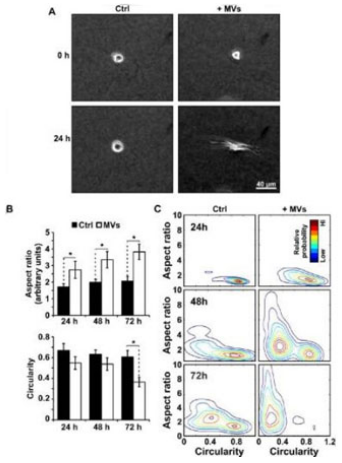


Figure
MVs induce morphological changes in epithelial cells cultured in 3D (A) Phase contrast images at 0 h and 24 h of MCF10a cells supplemented with MVs (+MVs) or culture media alone (Ctrl). (B) Corresponding quantification of aspect ratio and (C) circularity shape parameters measured from at least 60 cells from 3 independent experiments. Mean ± SE (D) Cell shape population distributions plotted as a function of the aspect ratio to circularity shape parameters. *p<0.05. Rat tail (p/n RT-T297). Fig 2. PMID: 26477404.

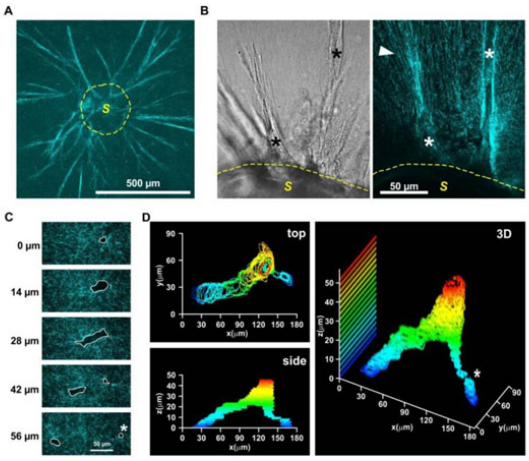


Figure
3D ECM remodeling by carcinoma-derived fibroblasts. (A) 3D reconstruction from confocal reflectance sections of a spheroid (S) composed of carcinoma-derived primary fibroblasts invading into a 3D collagen scaffolds. Cells were allowed to invade into the ECM for a period of 48 h. The original spheroid boundary is indicated by the dashed line. (B) Phase contrast image of the invading cells (indicated by the asterisks) and the corresponding confocal reflectance image showing the collagen remodeling perpendicular to the spheroid boundary (arrow). (C) Confocal reflectance images of collagen showing a Z stack of the microtrack left in the wake of a single cell migration due to ECM remodeling and (D) the corresponding 3D reconstruction of the microtrack. Rat tail (p/n RT-T297). Fig 4. PMID: 25866589.

References

- Korbmacher F et al. ETS-guided iPSC-endothelial models recapitulate malaria pathogenesis. *EMBO Mol Med.* (2026)
- Hu R et al. Protocol for studying dynamics of parasite-host-mediated endothelial inflammation in 3D engineered brain microvessels. *STAR Protoc.* (2025)
- Zanotelli, MR et al. Energetic costs regulated by cell mechanics and confinement are predictive of migration path during decision-making. *Nature Communications* (2019)
- Bernabeu, M et al. Binding Heterogeneity of Plasmodium falciparum to Engineered 3D Brain Microvessels Is Mediated by EPCR and ICAM-1. *MBio* (2019)
- Bordeleau, F et al. Microvesicles released from tumor cells disrupt epithelial cell morphology and contractility. *Journal of Biomechanics* (2016)
- Alcoser, TA et al. Probing the biophysical properties of primary breast tumor-derived fibroblasts. *Cellular and Molecular Bioengineering* (2015)

Disclaimer

This product is for research use only and is not intended for therapeutic or diagnostic applications. Please contact a technical service representative for more information. All products of animal origin manufactured by Rockland Immunochemicals are derived from starting materials of North American origin. Collection was performed in United States Department of Agriculture (USDA) inspected facilities and all materials have been inspected and certified to be free of disease and suitable for exportation. All properties listed are typical characteristics and are not specifications. All suggestions and data are offered in good faith but without guarantee as conditions and methods of use of our products are beyond our control. All claims must be made within 30 days following the date of delivery. The prospective user must determine the suitability of our materials before adopting them on a commercial scale. Suggested uses of our products are not recommendations to use our products in violation of any patent or as a license under any patent of Rockland Immunochemicals, Inc. If you require a commercial license to use this material and do not have one, then return this material, unopened to: Rockland Inc., P.O. BOX 5199, Limerick, Pennsylvania, USA.